

## Engineering of Ovonic Threshold Switching Selector: A Link from the Material Properties to the Electrical Performances

A. Verdy, M. Bernard, N. Castellani, P. Noé, C. Licitra, J. Garrione,  
G. Bourgeois, M. C. Cyrille and G. Navarro

CEA-LETI, Univ. Grenoble Alpes, 38000 Grenoble, France

**Abstract - We present the engineering of Ovonic Threshold Switching (OTS) selectors integrating Ge<sub>3</sub>Se<sub>7</sub> based alloys. We show how doping allows the tuning of the material properties and of the device performances, enabling to fulfill different applications' requirements. In particular, we show that, whereas an optimized Sb&N-doping leads to an ultra-low leakage current, As<sub>2</sub>Te<sub>3</sub>-doping enables tunable and predictable parameters over a wide range of compositions and thicknesses.**

### 1. Introduction

Crossbar Resistive Array (CRA) represents the main candidate for the development of Storage Class Memory. The leakage current  $I_{leak}$  and the sneak-paths, intrinsic to the parallelism of the CRA structure, require to add in series with the memory (1R) a selector device (1S). Selectors based on Ovonic Threshold Switching (OTS) mechanism [1] are considered today as good candidates among the different selector technologies, with already reliable demonstrations of co-integration with OxRAM [2,3] and PCM [4-6].

OTS materials are amorphous chalcogenide with the property to switch from a resistive state to a volatile conductive state, when the applied voltage reaches a threshold voltage  $V_{th}$ . The conductive state is sustained until the current is decreased below the holding current  $I_h$ . OTS selector requires a first initialization pulse, called firing, characterized by a higher switching voltage ( $V_{fire}$ ) than the following stable  $V_{th}$ , and by an increase of  $I_{leak}$  (measured at  $V_{th}/2$ ). Reading operation in 1S1R relies on an indirect measurement of the memory that requires to adapt the OTS threshold current  $I_{th}$  to the I-V characteristic of the high resistance state (HRS) of the memory [7]. Therefore, the functionality of the final 1R-1S device relies on a careful engineering of the OTS material to tune properly the selector electrical parameters.

In this paper, we present the engineering of OTS based on Ge<sub>3</sub>Se<sub>7</sub> (GS) alloy. We show how electrical parameters can be tuned by different dopants (Table 1), and we propose a benchmark between the different OTS materials developed.

### 2. Ultra-low leakage current in Sb&N-doped Ge<sub>3</sub>Se<sub>7</sub>

Doping GS with Sb to reduce  $V_{th}$  [8,9] induces the formation of Sb-Sb bonds (Fig. 1) that increases  $I_{leak}$  (Fig. 3), and degrades the thermal stability [9]. N-doping is known to improve the thermal stability of Ge-based chalcogenides [10]. By forming Ge-N bonds (Fig. 2) it permits to increase the glass rigidity and to suppress Sb-Sb bonds (Fig. 1), leading to very low  $I_{leak}$  and high thermal stability [7]. However, N-doping leads also to a high material disorder. Material reorganization upon thermal annealing at 400°C-30min occurs with the formation of a homogeneous GeN<sub>x</sub> phase, helping to decrease  $V_{fire}$  by keeping a very low leakage current (Fig. 3).

Sb&N-doped GS features an endurance of 10<sup>8</sup> cycles [11].

### 3. Tunable parameters in As<sub>2</sub>Te<sub>3</sub>-doped Ge<sub>3</sub>Se<sub>7</sub>

As<sub>2</sub>Te<sub>3</sub> (AT), like Sb, can be used to decrease the high  $V_{th}$  of GS. A limited chemical interaction between GS and AT (Fig. 4) leads to a linear decrease of  $E_g$  with AT content (Fig. 5). Thus, both  $V_{th}$  and  $I_{leak}$  can be modeled by simple equations relying respectively on the linear decrease of the threshold electric field with AT content, and a linear decrease of the activation energy of the electrical conduction, mainly driven by the Poole-Frenkel mechanism (Fig. 6). Therefore, the OTS electrical parameters can be predicted over a wide range of compositions and thicknesses allowing a fine-tuning of the alloy. Reliability of AT-doped GS is demonstrated by an endurance of more than 10<sup>10</sup> cycles [12].

### 4. Correlation between $E_g$ , $V_{fire}$ and $I_{leak}$

Optical bandgap  $E_g$  is extracted by means of Tauc plot extrapolation from ellipsometry measurements performed on Sb&N and AT doped GS as-deposited materials [9,13], representative of as-fabricated devices (i.e. before firing). We observe a linear correlation between  $V_{fire}$  and  $E_g$  (Fig. 7), and an exponential relation between  $I_{leak}$  and  $E_g$  (Fig. 8). These results show an intrinsic correlation between  $V_{fire}$  and  $I_{leak}$ , independent of the OTS composition (Fig. 9). However, OTS materials have also to deal with their stability against high temperature and electrical stress that can induce a degradation of the device performances, as an increase of  $I_{leak}$  after firing.

### 5. Benchmark of Ge<sub>3</sub>Se<sub>7</sub>-based OTS selectors

In Fig. 10 we compare the electrical parameters of different OTS selectors based on GS: AT-doped [12] and Sb&N-doped [13]. AT allows reducing  $V_{th}$  at values equivalent to the ones achieved by Sb, but featuring a lower  $I_{leak}$ . An optimized Sb&N-doping allows a moderate reduction of  $V_{th}$  but extremely low  $I_{leak}$ . Since Sb-doping shows high  $I_{th}$ , such materials are more suitable for a co-integration with a memory characterized by a low resistance in its HRS (high resistance state). On the contrary, Sb&N-doping (i.e. with the lowest  $I_{th}$ ) shows compatibility with 1R devices with higher HRS resistance. AT-doping permits to tune  $I_{th}$  between the values of Sb- and Sb&N-doping.

### 6. Conclusions

In this paper, we present the material engineering of OTS based on GS composition. The optimization of Sb- and N-doping in GS allows OTS selectors featuring extremely low  $I_{leak}$ . Then, tunable and predictable OTS electrical parameters are achieved by As<sub>2</sub>Te<sub>3</sub>-doping. We demonstrate the correlation between  $E_g$ ,  $V_{fire}$  and  $I_{leak}$ , showing that a reduction of  $V_{fire}$  implies an increase of  $I_{leak}$ . Finally, a benchmark between the different GS-based OTS selectors developed, demonstrates their suitability for different resistive memory technologies.

Name	Composition
GS	Ge <sub>3</sub> Se <sub>7</sub>
GSS	Sb-doped GS
GSSN	N-doped GS
AT	As <sub>2</sub> Te <sub>3</sub>
GS-AT	As <sub>2</sub> Te <sub>3</sub> -doped GS
Annealing: 400°C @ 30min	

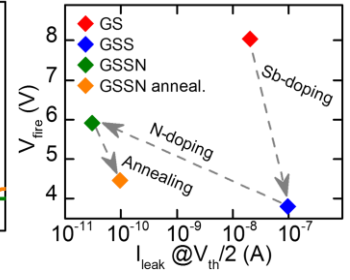
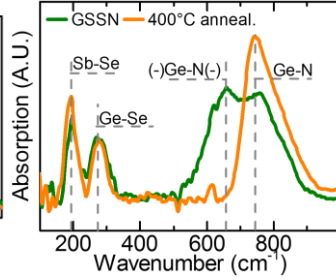
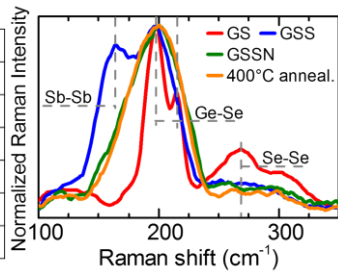


**Table 1:** Correspondence between alloys names used and OTS compositions

**Fig. 1:** Raman spectroscopy in Sb and/or N-doped GS alloys. An excess of Sb leads to the formation of Sb-Sb bonds that are suppressed by N-doping. After annealing, no material degradation occurs in GSSN.

**Fig. 2:** IR spectroscopy highlighting the formation of Sb-Se and Ge-N bonds. After the annealing, a homogeneous GeN<sub>x</sub> phase appears.

**Fig. 3:** Sb-doping helps to decrease V<sub>fire</sub> at the expense of a I<sub>leak</sub> increase. N-doping helps to decrease I<sub>leak</sub> but with an increase of V<sub>fire</sub>. The Annealing decreases V<sub>fire</sub>, while keeping a very low I<sub>leak</sub>.

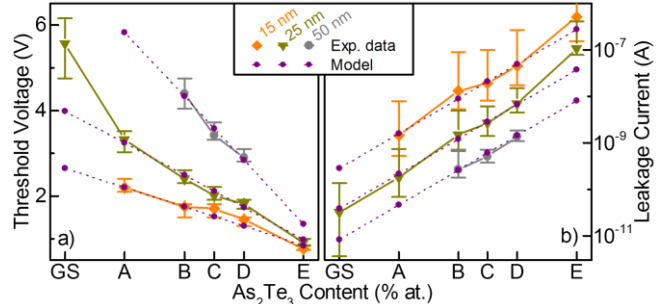
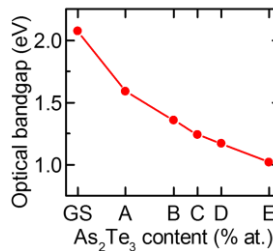
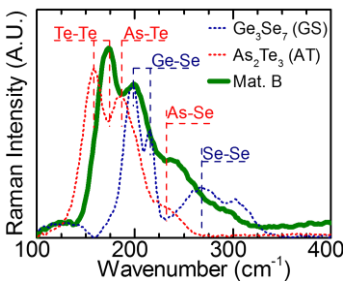


**Fig. 5:** In GS + AT alloys, the local orders of both GS and AT systems coexist, indicating that a limited chemical interaction occurs between the two alloys.

**Fig. 6:** The optical bandgap of AT-doped alloys linearly decreases with AT content.

**Fig. 4:** Experimental data and fitting of a) threshold voltage V<sub>th</sub> and b) leakage current I<sub>leak</sub> for different compositions and thicknesses. Electrical parameters in GS-AT alloys can be predicted by simple relations thanks to the linear decrease of E<sub>g</sub> with AT content. It is helpful to finely tune the OTS electrical parameters.

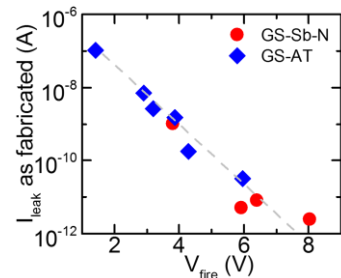
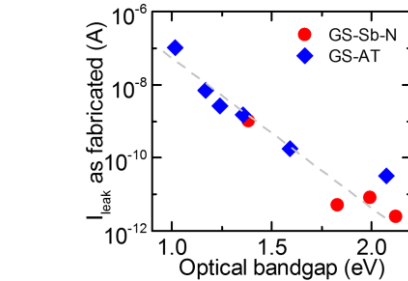
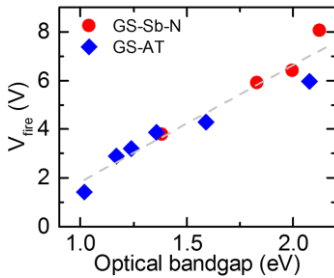


**Fig. 7:** Evolution of V<sub>fire</sub> as a function of E<sub>g</sub> for different compositions. A linear correlation is observed. Data for Sb&N-doped GS (GS-Sb-N) are from [13].

**Fig. 8:** Evolution of I<sub>leak</sub> on as-fabricated devices as a function of E<sub>g</sub>. I<sub>leak</sub> increases exponentially with E<sub>g</sub>, compatibly with a Poole-Frenkel electrical conduction (data for GS-Sb-N are from [13]).

**Fig. 9:** Correlation between V<sub>fire</sub> and I<sub>leak</sub>. Decrease of V<sub>fire</sub> induces an increase of I<sub>leak</sub> (i.e. both parameters depend on E<sub>g</sub>).

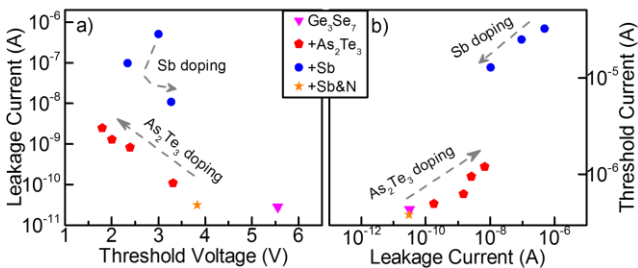


**Fig. 10:** Benchmark of a) I<sub>leak</sub> vs V<sub>th</sub> and b) I<sub>leak</sub> vs I<sub>th</sub> for different dopants in GS: AT, Sb and Sb&N [12]. The lowest I<sub>leak</sub> is achieved with Sb&N-doping. AT allows the same V<sub>th</sub> as Sb with the advantage of a lower I<sub>leak</sub>. Sb allows the highest I<sub>th</sub>, making Sb-doping suitable for memory with low HRS resistance. On the contrary, low I<sub>th</sub> in Sb&N-doped GS is suitable for devices with high HRS resistance. I<sub>th</sub> can be tuned with AT-doping between the values of Sb- and Sb&N- doping.

## References

- [1] S. R. Ovshinsky, Phys. Rev. Lett., vol.21 (20), 1968.
- [2] M. Alayan et al., 2017 IEEE IEDM, pp.2.3.1-2.3.4, 2017.
- [3] D. Alfaro Robayo et al., 2019 IEEE IMW, pp. 132-135, 2019.
- [4] G. Navarro et al., 2017 IEEE VLSI, pp. T94-T95, 2017.
- [5] T. Kim et al., 2018 IEEE IEDM, pp. 37.1.1-37.1.4, 2018.
- [6] <http://www.techinsights.com/about-techinsights/overview/blog/intel-3D-xpoint-memory-die-removed-from-intel-optane-pcm/>
- [7] A. Verdy et al., 2018 IEEE IEDM, pp. 37.4.1-37.4.5, 2018.
- [8] S.-D. Kim et al, ECS Solid State Lett., vol. 2, pp.Q75-Q77, 2013.
- [9] A. Verdy et al., 2017 IEEE IMW, pp. 84-87, 2017.
- [10] A. Fantini et al., 2010 IEEE IEDM, pp. 644-647, 2010.
- [11] A. Verdy et al., 2018 IEEE IMW, 2018.
- [12] A. Verdy et al., 2019 IEEE IMW, pp. 79-92, 2019.
- [13] A. Verdy et al., 2018 MRS Spring Meeting, 2018.

## Acknowledgements

This work has been partially supported by the European 621217 PANACHE project and 783176 WAKeMeUP project.